Temporal Variability of Polycyclic Aromatic Hydrocarbons in Deep-Sea Cephalopods of the Northern Gulf of Mexico

Isabel C. Romero[1]*, Heather Judkins[2] and Michael Vecchione[3]

[1] College of Marine Science, University of South Florida, Tampa, FL, United States, [2] Biological Sciences Department, University of South Florida St. Petersburg, St. Petersburg, FL, United States, [3] NMFS National Systematics Laboratory, National Museum of Natural History, Washington, DC, United States

As part of the effort to understand the effects of the Deepwater Horizon Oil Spill (DWHOS), we analyzed tissue from five species of midwater oceanic cephalopods in the northern Gulf of Mexico (GoM) during three time periods, including one period sampled fortuitously just before the spill (2010), and two periods sampled after the spill (2011 and 2015–2016). The species, *Japetella diaphana*, *Abralia redfieldi*, *Histioteuthis corona*, *Leachia atlantica*, and *Onychoteuthis banksii* were collected in three geographic areas in the GoM (east, south and southeast of the Macondo wellhead). Results indicate a shift in the composition of polycyclic aromatic hydrocarbons (PAHs) in the tissue of all cephalopods after 2010, with a more petrogenic source in 2011 that weathered and mixed with other sources in 2015–2016. Overall, PAH concentrations, as well as lipid content, were lower in 2011 relative to 2010 and 2015–2016, suggesting secondary effects to oil-residues exposure from the DWHOS. Collectively, PAHs in the tissues of deep-sea cephalopods indicate an episodic exposure to petrogenic PAHs that occurred between 2010 (pre-spill) and 2011, and continued through 2015–2016.

Keywords: oil spills, exposure to oil contamination, oil-residues, long-term effects, deepwater horizon spill

INTRODUCTION

Ecosystem-based management of the oceans relies heavily on continuous observations, essential for distinguishing natural variability from anthropogenic changes. However, epi-, meso-, and bathy-pelagic environments generally lack such studies. This was highlighted in 2010 by the absence of baseline data during the Deepwater Horizon oil spill (DWHOS) in the Gulf of Mexico (GoM). The DWHOS occurred at a depth of 1500 m, releasing approximately 4000000 barrels of oil that contaminated vast areas of the water column (e.g., oil residues rose to form surface slicks contaminating the water column, subsurface plumes concentrated at 900–1300 m) and coastal environments (e.g., marshes, beaches), as well as an extensive area of the seafloor (about 76000 km^2 by sinking of oil residues from the water column) (Dietrich et al., 2012; Brooks et al., 2015; MacDonald et al., 2015; Romero et al., 2015, 2017; Daly et al., 2016; Harding et al., 2016; Murawski et al., 2016; Yan et al., 2016). The deep-pelagic habitat in the GoM was among the environments most affected by the DWHOS, as indicated by multiple studies detecting high concentration of contaminants and shifts in the composition of microbial communities (Hazen et al., 2010;

Fisher et al., 2016; Wade et al., 2016; Yan et al., 2016). Effects to marine communities were observed as carbon from the DWHOS entered the planktonic and mesopelagic food webs, and oil-derived toxic compounds were found to correlate with elevated skin lesions in bottom-dwelling offshore fishes (Graham et al., 2010; Chanton et al., 2012; Murawski et al., 2014; Quintana-Rizzo et al., 2015). Oil residues from the DWHOS have persisted in the deep-pelagic habitat of the GoM longer than anticipated. For example, 4–6 years after the DWHOS as found in the water column and in deep-pelagic fishes (Walker et al., 2017; Chanton et al., 2018; Romero et al., 2018). The potential consequences of the DWHOS on deep-pelagic invertebrates are yet to be determined, as exposure to oil-derived toxic compounds has not been previously studied in invertebrates from the pelagic domain of the GoM.

Many deep-sea pelagic organisms undergo diel vertical migrations, playing an important role in the flux of organic carbon between the surface and bathypelagic depths, including the water column and benthic ecosystems (Steinberg et al., 2008; Davison et al., 2013; Hudson et al., 2014; Irigoien et al., 2014; Steinberg and Landry, 2017; Taucher et al., 2018). Deep-sea cephalopod species are of particular interest due to their role in the diets of large fishes and marine mammals (Davis et al., 2007; Young et al., 2010; Romeo et al., 2012; Logan et al., 2013; Lalas and Webster, 2014; Salman and Karakulak, 2019; Southall et al., 2019). They are also voracious predators (Stewart et al., 2014; Corrales et al., 2015; Hoving and Robison, 2017) and are therefore potential vectors for contaminants through the water column (Unger et al., 2008).

Exposure to toxic compounds, such as polycyclic aromatic hydrocarbons (PAHs), is of specific concern in deep-pelagic cephalopods. These toxic compounds are highly lipid-soluble and therefore can cross lipid membranes and bioaccumulate in marine organisms. Mollusks, including cephalopods, have a reduced capacity to metabolize PAHs with higher bioaccumulation potential than other aquatic organisms (Lacoue-Labarthe et al., 2016; Rodrigo and Costa, 2017). In addition, cephalopods have high growth rates, short life spans, and high sensitivity to environmental changes (Rodrigo and Costa, 2017). Cephalopods have a high capacity to bioaccumulate and concentrate contaminants at higher levels than other aquatic groups, thus are potentially useful bioindicators of aquatic contamination over short periods (Gomes et al., 2013; Semedo et al., 2014). During the DWHOS, an unprecedented amount of PAHs was released, with PAHs remaining mostly offshore and contaminating the deep-pelagic domain of the northern GoM (U.S. District Court, 2015; Wade et al., 2016; Romero et al., 2017, 2018). However, comprehensive studies of PAHs in cephalopod tissues are scarce, with little understanding of the influence of natural and biological factors (e.g., diet, migratory behavior, habitat) affecting their storage after major events like the DWHOS.

This study investigated, for the first time, the composition and concentration of PAHs in deep-sea cephalopods of the GoM over a long period, to better understand levels of contamination, interspecies variability, exposure to natural sources, and potential consequences to the deep-pelagic environment. Specifically,

samples were collected before and up to 6 years after the DWHOS (pre-spill: 2010, post-spill: 2011, long-term period: 2015–2016). The samples collected before the DWHOS (January to March, 2010), provided an exceptional opportunity to study uptake and persistence of petrogenic PAHs under multiple natural and anthropogenic sources present in the GoM (Mitra et al., 2002; Mitra and Bianchi, 2003; Romero et al., 2016). Overall, this study provides a time-series analysis of PAH composition and concentrations generating trends in PAH signatures for baseline and chronic conditions in deep-sea cephalopods.
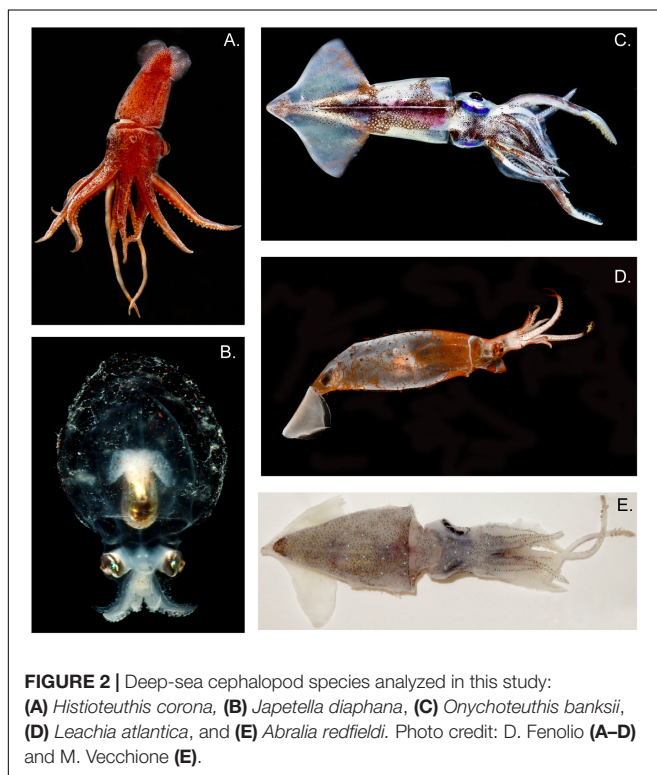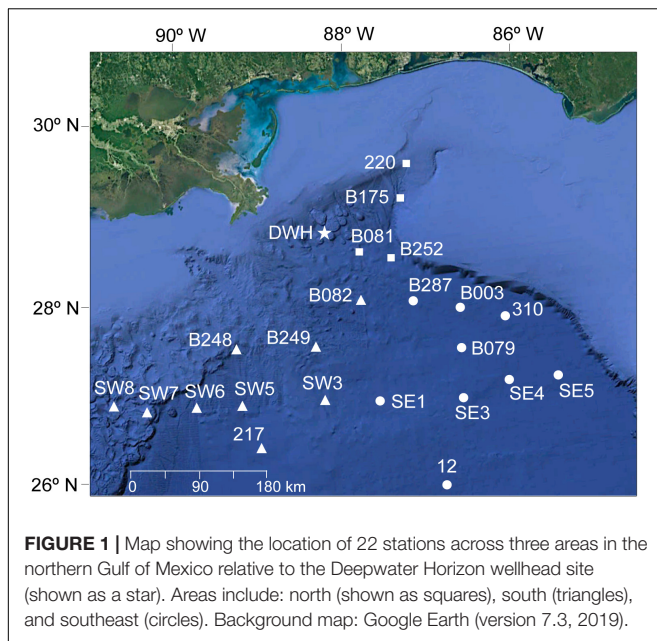
MATERIALS AND METHODS

Collection of Samples

Samples were collected during three different studies conducted between 2010 and 2016. In all studies, trawl samples were collected within the upper 1500 m of the water column. In 2010, sampling was conducted from January to March aboard the NOAA Ship R/V *Pisces* for the Sperm Whale Acoustic Prey Survey (SWAPS; see Judkins et al., 2015) using a large midwater trawl. In 2011, sampling was conducted from March to September aboard the R/V *Meg Skansi* as part of the Offshore Nekton Sampling and Analysis Program (ONSAP) using a 10-m^2 MOCNESS (MOC10) with 3-mm mesh (Judkins et al., 2017). In 2015 and 2016, sampling was conducted in May and August aboard the R/V *Point Sur* as part of the Deep Pelagic Nekton Dynamics of the Gulf of Mexico (DEEPEND), also using a MOC10. All studies covered similar sites in the northern GoM (**Figure 1**). The spatial range of these studies extended from 24.4 to 29.3° N latitude and 86.5 to 90.9° W longitude (**Figure 1**). Sampling stations were located in three areas in the northern GoM relative to the Macondo wellhead, similar to previous studies in the region (Judkins et al., 2017; Romero et al., 2018). In the east area, four stations were sampled, located between ~41 and ~123 km east of the wellhead. In the south area, ten stations were sampled, located between ~88 and ~312 km south of the wellhead. In the southeast area, eight stations were sampled, located between ~120 and ~297 km southeast of the wellhead. All areas were sampled between 2010 and 2016, except for the southeast area (only during 2010 and 2015–2016).

Taxonomic identification of all samples was highly consistent among studies. All specimens were identified to the lowest taxonomic level possible, by either H. Judkins or M. Vecchione while at sea. Deep-sea cephalopod species that were available for chemical analysis and included in this study are *Japetella diaphana* (n = 18), *Abralia redfieldi* (n = 11), *Histioteuthis corona* (n = 11), *Leachia atlantica* (n = 21), and *Onychoteuthis banksii* (n = 13) (**Figure 2**). PAH exposure and accumulation was studied as PAH concentrations in the mantle tissue. A small piece of mantle tissue was taken from the anterior portion of the mantle and samples were kept frozen at −20°C until freeze-dried.

Lipid Extraction

Frozen mantle tissue was freeze-dried (Labonco® 7754040 vacuum freeze-drier and 7806020 bulk tray) following guidance from previous studies (Beriro et al., 2014; Romero et al., 2018).

FIGURE 1 | Map showing the location of 22 stations across three areas in the northern Gulf of Mexico relative to the Deepwater Horizon wellhead site (shown as a star). Areas include: north (shown as squares), south (triangles), and southeast (circles). Background map: Google Earth (version 7.3, 2019).

FIGURE 2 | Deep-sea cephalopod species analyzed in this study: (A) *Histioteuthis corona*, (B) *Japetella diaphana*, (C) *Onychoteuthis banksii*, (D) *Leachia atlantica*, and (E) *Abralia redfieldi*. Photo credit: D. Fenolio (A–D) and M. Vecchione (E).

Freeze-dried samples were ground to homogenize the tissue, which was then extracted using an Accelerated Solvent Extraction system (ASE 200®, Dionex) under high temperature (100°C) and pressure (1500 psi) with a solvent mixture of 9:1 (v:v) hexane:dichloromethane. Deuterated PAHs (d$_{10}$-acenaphthene, d$_{10}$-phenanthrene, d$_{10}$-fluoranthene, d$_{12}$-benz(a)anthracene, d$_{12}$-benzo(a)pyrene, d$_{14}$-dibenz(ah)anthracene; Ultra Scientific ISM-750-1) were added to samples prior to extraction as surrogate standards. A one-step extraction and clean-up procedure was applied using 11 ml extraction cells with glass fiber filters (pre-combusted at 450°C for 4 h), 5 g silica gel (high purity grade, 100–200 mesh, pore size 30A, Sigma Aldrich, United States; pre-combusted at 450°C for 4 h, and deactivated 2%), sand (pre-combusted at 450°C for 4 h), and 0.01–0.1 g freeze-dried homogenized sample (Romero et al., 2018). Tissue extracts were concentrated to ∼100–200 µl using a RapidVap (LABONCO RapidVap® Vertex^{TM} evaporator model 73200 series) and a gentle stream of nitrogen. Two extraction control blanks were included with each set of samples (10–14 samples). An internal standard was added (d14-terphenyl; Ultra Scientific ATS-160-1) to all samples prior to GC/MS analysis. All solvents used were at the highest purity available.

Total lipid content (TLC; %lipids) in tissue was calculated gravimetrically from ASE extracts using 100% dichloromethane (Sloan et al., 2004) in samples with sufficient mass available (∼0.5 g) after PAH analysis. For samples with limited mass after PAH extraction, we followed modified gas chromatography method (Hooper and Parrish, 2009) to calculate the %lipid as the total lipid-equivalent fraction by calculating the sum of individual lipids to generate an estimate of total lipids (see Romero et al., 2018, for details).

Analytical Method and Quality Control

We followed modified EPA methods 8270D and 8015C, and QA/QC protocols for the analysis of PAHs. Analyses were carried out on an Agilent 7680B gas chromatograph interfaced with an Agilent 7010 triple quadrupole mass spectrometer (GC/MS/MS). A 30 m RXi-5sil (Restek Corporation, PA, United States) was used with GC liners in the injector in splitless injection mode. UHP helium was used as the carrier gas, while UHP argon gas was used to facilitate the dissociation of the precursor ions (CID) in the collision cell (at 1 mTorr pressure). Inlet temperature was 295°C, constant flow rate was 1 ml/min, and MS detector temperature was 250°C. GC oven temperature program was 60°C for 2 min, 60°C to 200°C at a rate of 8°C/min, 200°C to 300°C at a rate of 4°C/min and held for 4 min, and 300°C to 325°C at a rate of 10°C/min and held for 5 min.

The GC/MS/MS was operated in Multiple Reaction Monitoring mode (MRM) to characterize parent and alkyl PAHs at a high resolution without interferences in the chromatograms. Molecular ion masses for PAHs (precursor and product ions) were selected based on previous studies using GC-MS/MS-MRM (Sorensen et al., 2016; Adhikari et al., 2017; Romero et al., 2018; van Eenennaam et al., 2018). Selected target compounds were 2-ring PAHs: naphthalene (N) and alkylated homologs (N C1-C4); 3-ring: acenaphthylene (ACL), acenaphthene (ACE), fluorene (F), dibenzothiophene (D), phenanthrene (P), anthracene (AN), and their alkylated homologs (P/AN C1-C4, D C1-C2); 4-ring: fluoranthene (FL), pyrene (PY), benz[a]anthracene (BAA), chrysene (C), and their alkylated homologs (FL/PY C1-C4, BAA/C C1-C4); 5-ring: benzo[b]fluoranthene (BBF), benzo[k]fluoranthene (BKF), benzo[a]pyrene (BAP), dibenz[a,h]anthracene (DA), and alkylated homologs (BP/PER C1-C4); and 6-ring: indeno[1,2,3-cd]pyrene (ID), benzo[ghi]perylene (BGP).

For accuracy and precision of analyses we included laboratory blanks for every 10–14 samples, spiked controls for every 14–18 samples, tuned MS/MS to PFTBA (perfluorotributylamine) daily, checked samples with a standard reference material (NIST 2779) daily, and reanalyzed sample batches when replicated standards exceeded ±20% of relative standard deviation (RSD), and/or when recoveries were low. Recovery of individual PAHs ranged within QA/QC criteria of 50–120%. PAH concentrations are reported as recovery corrected. Each PAH analyte was identified using certified standards (Chiron S-4083-K-T, Chiron S-4406-200-T) and performance was checked using a 5-point calibration curve (0.04, 0.08, 0.31, 1.0 ppm). Quantitative determination of PAHs was conducted using response factors (RFs) calculated from the certified standard NIST2779. The limits of quantification and detection ($N = 10$) ranged from 0.01 to 0.9 ng/g and 0.001 to 0.3 ng/g, respectively.

Data Analysis

Polycyclic aromatic hydrocarbons concentrations reported in this study are expressed as tissue lipid weight concentrations, and average values are shown as arithmetic mean ± standard error. Total PAH concentrations were calculated as the sum of 2-ring to 6-ring PAHs and their alkylated homologs. Low molecular weight (LMW) PAHs are the sum of all 2–3 ring PAHs (including alkylated homologs), and high molecular weight (HMW) PAHs are the sum of 4–6 ring PAHs (including alkylated homologs). To assess sources of PAHs in the tissue samples, selected diagnostic ratios were calculated: (1) FL/Pyr ratio; (2) % Retene; and (3) pyrogenic index [PI; Σ (other 3–6 ring EPA priority PAHs)/Σ(5 alkylated PAHs)]. For the pyrogenic index, the five alkylated PAHs are the alkylated compounds of: N, P, D, F, and C. The "other" 3–6 ring EPA priority PAHs are: ACL, ACE, AN, FL, PY, BAA, BBF, BKF, BAP, ID, DA, and BGP (Wang and Fingas, 2003; Fitzgerald and Gohlke, 2014; Romero et al., 2015, 2018). These PAH ratios include isomer pairs with similar adsorption and dissolution properties abundant in different sources.

Statistical analyses were conducted on log-transformed data to approach normal distribution. Differences in mean concentrations with respect to years and species were tested by one-way ANOVA followed by Tukey's HSD test. Significance was set at $p < 0.05$. We used JMP 12.1 for Mac (SAS Institute Inc., Cary, NC, United Sates, 1989–2007).

RESULTS

Species Variability

Large variability among cephalopod species was found for %lipid content and PAH concentrations over the studied period (**Figure 3**). For example, %lipid content varied significantly among the species studied, although a similar temporal trend was observed with lower %lipid content in 2011 (post-spill) for all species sampled in this year ($p < 0.05$; *J. diaphana*: 4.0 ± 0.8%; *A. redfieldi*: 7.2 ± 1.6%; *H. corona*: 11.8 ± 1.3%; *L. atlantica*: 5.6 ± 0.6%; and *O. banksii*: 6.1 ± 0.5%; **Figure 3**). Lipid loss in 2011 relative to 2010 (pre-spill) was about 50% in *J. diaphana* and *L. atlantica*, and about 25% in *A. redfieldi* and *H. corona*.
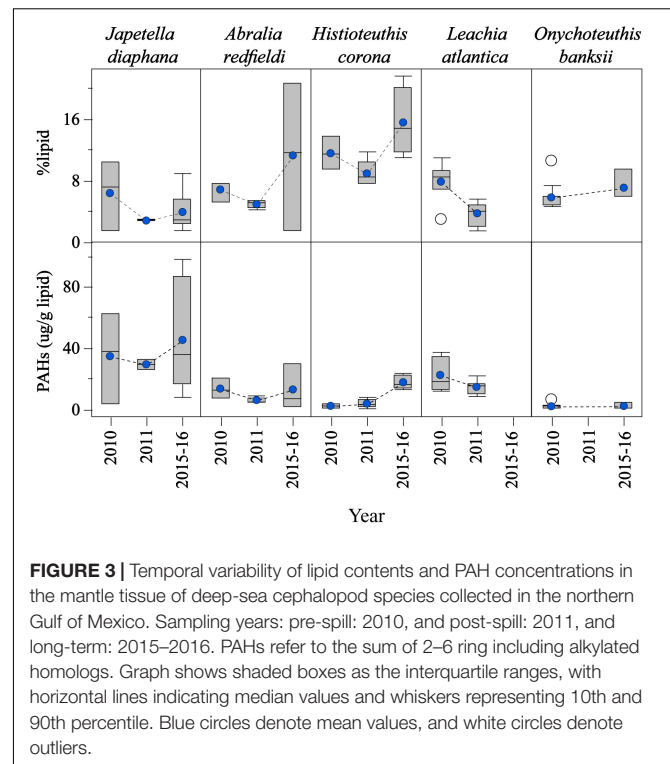

FIGURE 3 | Temporal variability of lipid contents and PAH concentrations in the mantle tissue of deep-sea cephalopod species collected in the northern Gulf of Mexico. Sampling years: pre-spill: 2010, and post-spill: 2011, and long-term: 2015–2016. PAHs refer to the sum of 2–6 ring including alkylated homologs. Graph shows shaded boxes as the interquartile ranges, with horizontal lines indicating median values and whiskers representing 10th and 90th percentile. Blue circles denote mean values, and white circles denote outliers.

An increase in %lipid content was observed in 2015–2016 for all species sampled in the long-term period (**Figure 3**).

Due to the differences found in %lipid content among the species studied, PAH concentrations were calculated as lipid-normalized concentrations (μg PAH/g lipid weight). PAH concentrations were lower post-spill for *J. diaphana*, *A. redfieldi*, and *L. atlantica*, with 16%, 56%, 34% decrease in PAH concentration in 2011 relative to 2010, respectively (**Figure 3**). *Histioteuthis corona* showed lower PAH concentrations in 2010 (pre-spill) and 2011 (post-spill), with a ∼84% increase in concentration during 2015–2016 (long-term period; **Figure 3**). In contrast, *O. banksii* showed similar PAH concentrations between the pre-spill and long-term periods (**Figure 3**). The temporal trend in PAH concentration observed in most species is not explained by %lipid content because lipid-normalized PAH data removes the influence of interspecies %lipid content. Also, we found that PAH concentrations were not correlated with mantle length in all cephalopod species ($p > 0.05$), except *H. corona* ($R^2 = 0.011$; $p < 0.01$; **Table 1**). However, significant differences of PAH concentrations between cephalopod life stages were not found in any studied year for any species, including for *H. corona* ($p > 0.05$; **Table 1**). Therefore, the temporal trend in PAH concentration for *H. corona* is not explained by the different lengths of animals collected among the years.

A similar abundance of 3-ring (76 – 81% phenanthrene compounds, including alkyl homologs) and 4-ring (11 – 17% pyrene and fluoranthene compounds, including alkyl homologs) PAHs were observed among the species studied (**Figure 4**). However, small changes in the composition of PAHs were detected between the periods covered in this study (**Figure 4** and

TABLE 1 | Temporal variability of PAH concentrations (µg/g lipid weight) in mantle tissue of mature and immature deep-sea cephalopods from the northern GoM.

Species	Life stages	n	Collection period		
			2010	**2011**	**2015–2016**
Japetella diaphana	Immature	4	37.7	32.1	30.1 ± 13.9
	Mature	14	32.9 ± 29.6	26.2	48.4 ± 12.0
Histioteuthis corona	Immature	5	N.A.	4.2	17.5 ± 2.2
	Mature	6	2.0 ± 1.0	3.0 ± 1.6	N.A.
Abralia redfieldi	Immature	2	N.A.	N.A.	15.5 ± 13.9
	Mature	9	13.3 ± 3.9	5.8 ± 0.9	7.2
Leachia atlantica	Mature	21	22.2 ± 3.4	14.4 ± 1.4	N.A.
Onychoteuthis banksii	Immature	1	N.A.	N.A.	4.4
	Mature	12	1.8 ± 0.6	N.A.	0.7 ± 0.4

Studied periods: pre-pill (2010), post-spill (2011), long-term (2015–2016). Data are shown as mean ±SE.

Supplementary Figure S1). In 2010 (pre-spill), PAH composition indicates a dominant petrogenic source in all species except *O. banksii* with a strong signature of pyrogenic PAHs (from probable combustion products). In 2011 (post-spill), a small change was observed with an increase in the abundance of 2–3 ring and alkyl PAHs (up to ~20%). The small shift in the composition of PAHs indicates a larger source of low molecular weight PAHs post-spill (2011) for *A. redfieldi*, *L. atlantica* and *O. banksii* (typical distribution of %lipid abundance in the order of C0 < C1 < C2 > C3 > C4). Species like *H. corona* and *J. diaphana* showed a decrease in low molecular weight PAHs and an increase in alkyl PAHs post-spill, that may be related to their different behavior in the water column (see section "Discussion"). Altogether, the changes observed in the composition of PAHs indicate a different source after the spill that mixed with other sources over time (e.g., pyrogenic, seeps), like indicated by the composition of PAHs during the long-term period (2015–2016; **Figure 4**, **Supplementary Figure S1**).

Spatial Variability of PAHs

In 2010 (pre-spill), significantly lower PAH concentrations were observed in the south area relative to the other areas ($p < 0.001$; east: 15.9 ± 6.4 µg/g lipid; south: 4.5 ± 3.7 µg/g lipid; southeast: 18.9 ± 4.7 µg/g lipid). In contrast, in 2015–2016 (long-term period), PAH concentrations were not significantly different among the areas studied ($p > 0.05$). Only the south area showed significant differences in PAH concentrations in the tissue samples among years ($p < 0.001$), with an increase of PAHs over time (**Supplementary Figure S2**). The composition of PAHs changed post-spill (2011) and returned during the long-term period to conditions similar to pre-spill (**Supplementary Figure S3**). These results indicate that the temporal trend observed in the concentration and composition of PAHs is independent of the area sampled in each time period.
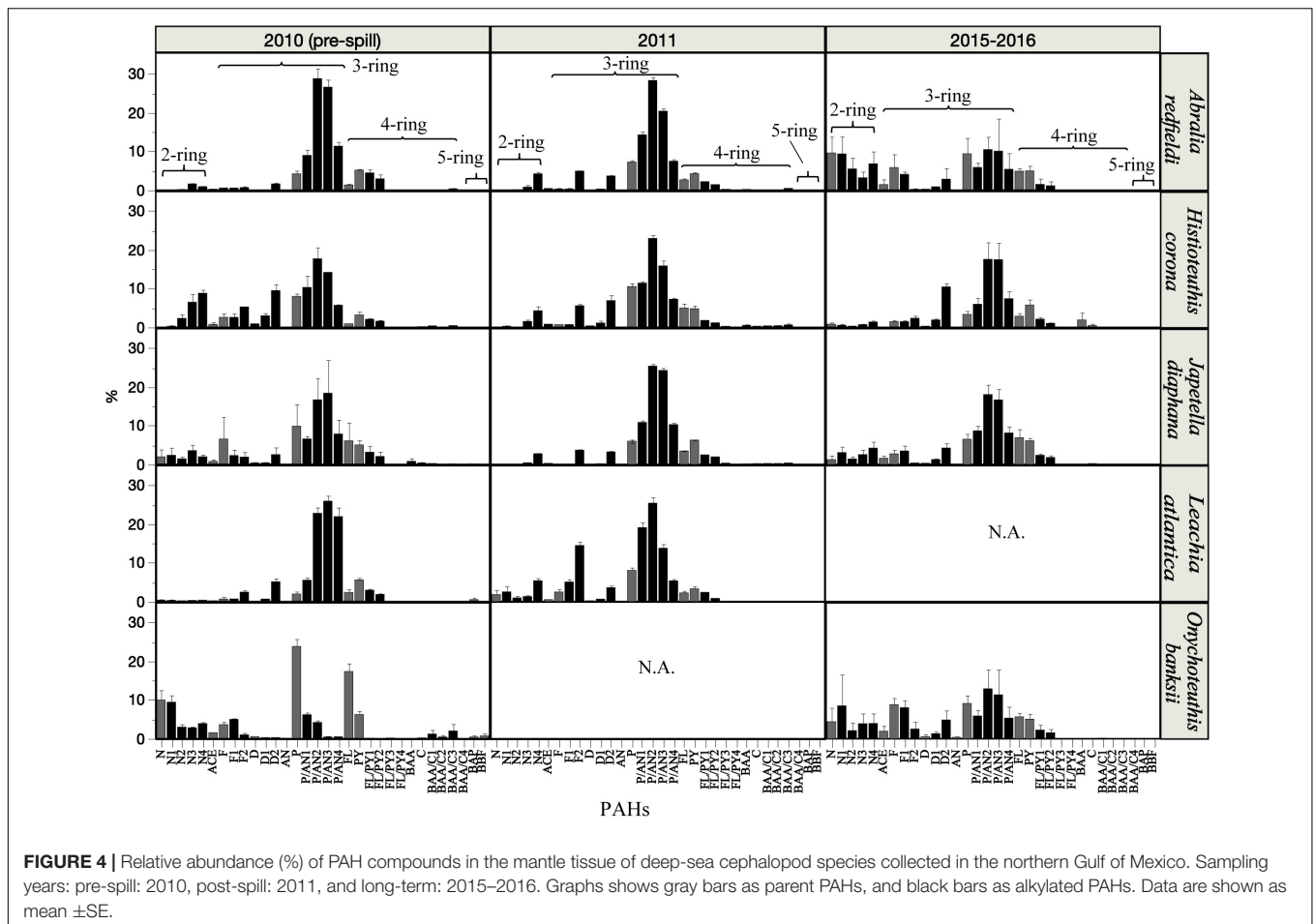
General Temporal Trends in PAH Levels and Composition

Even though a large variability was observed among the cephalopod species studied, all species indicate a higher exposure to 2–3 ring PAHs after 2010 (**Figure 4**). By integrating the PAH data from all species together, the general temporal trend observed indicates a ~2-fold increase in PAH concentrations during the long-term period relative to samples collected pre-spill for the deep-sea cephalopod assemblage in the northern GoM (2010: 13.5 ± 3.0 µg/g lipid weight; 2011: 11.5 ± 1.7 µg/g lipid weight; and 2015–2016: 29.0 ± 6.6 µg/g lipid weight). Significantly higher concentrations were consistently observed in the long-term period relative to the pre-spill and post-spill periods ($p < 0.01$; **Figure 5**). Collectively, the trends observed in PAH composition and calculated ratios suggest an episodic exposure to petrogenic PAHs that occurred after the post-spill period (2011) and continue through 2016 ($p < 0.01$; **Figures 6, 7**). In 2010 (pre-spill), higher ratios denote a more pyrogenic origin for PAHs (higher combustion sources) (HMW: 19.3 ± 2.0%; FL/Pyr: 1.5 ± 0.3; PI: 0.4 ± 0.1). In contrast, lower PAH ratios in 2011 (post-spill), indicate a petrogenic source (HMW: 11.5 ± 0.9%; FL/Pyr: 0.9 ± 0.1; PI: 0.1 ± 0.01). A slight increase in PAH ratios during the long-term period (2015–2016) indicate weathered oil-residues (more alkyl PAH compounds), as expected 5–6 years after the DWHOS (HMW: 15.9 ± 1.7%; FL/Pyr: 1.1 ± 0.2; PI: 0.3 ± 0.01). A similar %lipid abundance of retene (a 3-ring PAH) among sampling periods ($p > 0.05$) indicates a consistently low source of natural PAHs to the deep-pelagic environment during this study (2010–2016).

DISCUSSION

Interspecies differences were observed in lipid content and PAH concentrations, suggesting biological factors (e.g., diet, habitat, life span, behavior, and lipid metabolism) play an important role in the bioaccumulation of PAHs in the mantle tissues (**Table 1**). The species examined in this study are different from one another in many physical and ecological aspects (**Supplementary Table S1**). *Abralia redfieldi* is a small muscular squid (collected sizes: 9–35 mm ML), living primarily in the mesopelagic and migrating to the epipelagic zone nightly (Judkins and Vecchione, this vol.). *Onychoteuthis banksii* is also a muscular squid, but larger (collected sizes: 14–326 mm ML) and found at depth during the day and migrating to the upper mesopelagic and epipelagic zones nightly. In contrast, *J. diaphana* is a gelatinous octopod (collected sizes: 9–105 mm ML), found throughout the water column from the epi- to the bathy-pelagic zones; it exhibits ontogenic descent (i.e., larger individuals tend to live deeper in the water column than smaller ones). *Leachia atlantica* is a glass squid species (collected sizes: 36–111 mm ML) that uses an ammonia-filled chamber to achieve neutral buoyancy and it is found throughout the water column with no evidence of ontogenic descent (Judkins and Vecchione, this vol.). Very different from the other species studied, *H. corona* is a large squid with ammoniacal muscle tissue (collected sizes: 17–71 mm ML; max known size: ~190 mm ML) that does not vertically migrate daily, primarily inhabiting the mesopelagic zone. Altogether, these multiple ecological differences might affect lipid content and PAH concentrations among the species studied (**Figure 3**), as species are exposed to different environments in the water
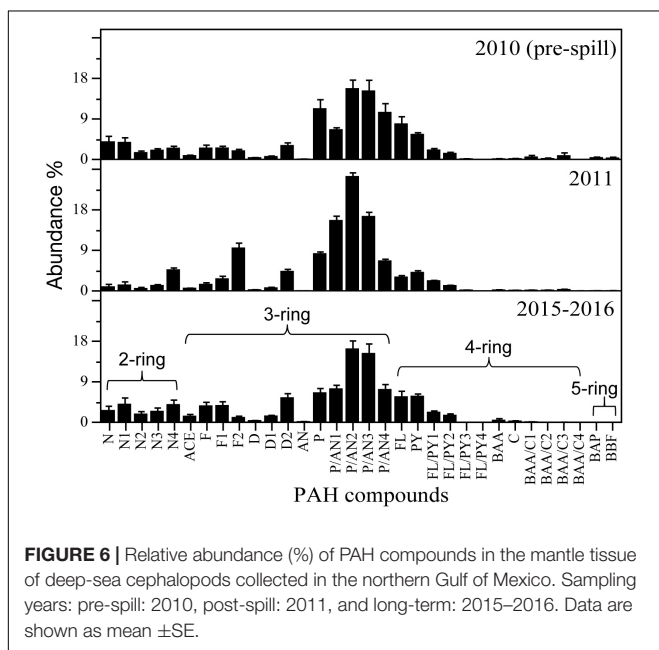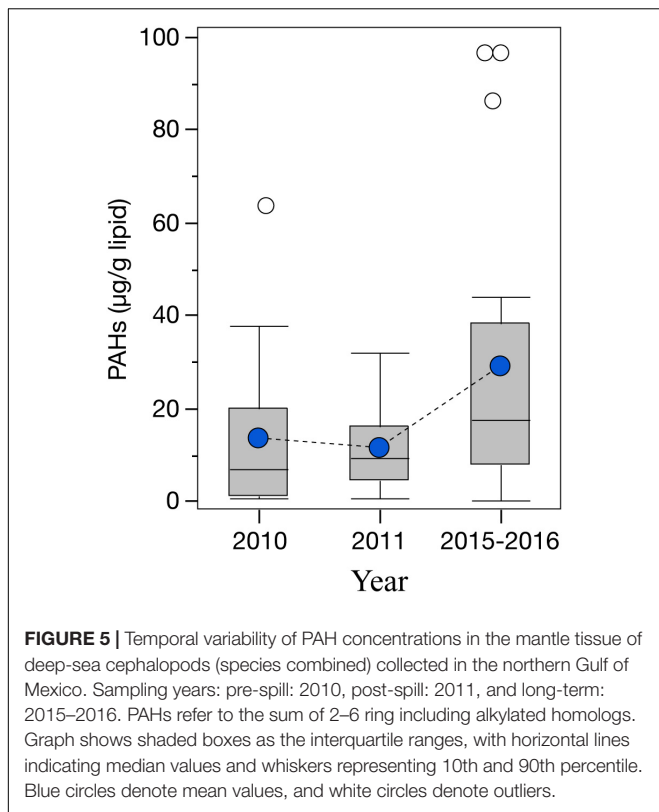
FIGURE 4 | Relative abundance (%) of PAH compounds in the mantle tissue of deep-sea cephalopod species collected in the northern Gulf of Mexico. Sampling years: pre-spill: 2010, post-spill: 2011, and long-term: 2015–2016. Graphs shows gray bars as parent PAHs, and black bars as alkylated PAHs. Data are shown as mean ±SE.

column. For example, *H. corona* and *J. diaphana* do not migrate vertically every day to the surface (∼50 m). Therefore, they may have been exposed to different hydrocarbon mixtures formed in the water column after released at ∼1500 m depth containing distinct chemical compositions (Ryerson et al., 2012). Also, biological parameters such as lipid metabolism may have an essential role in the variability of PAH bioaccumulation among cephalopod species. It seems that in some shallower-living cephalopod species, the digestive gland has an important role in detoxification of organic pollutants, including PAHs (Rodrigo and Costa, 2017). The physiological and molecular mechanisms involved in detoxification processes for organic pollutants in deep-sea cephalopod species are not known. It seems likely that the pathways for detoxification of organic pollutants may be different among the deep-sea cephalopod species studied as shown by the PAH concentrations in the mantle tissues (**Figure 3**).

Interestingly, the temporal trends observed in this study were all similar among the deep-sea cephalopod species studied. For example, our results indicate a shift in the composition of PAHs in all cephalopod species in 2011 (post-spill) relative to 2010 (January to March; pre-spill) that continue to 2015–2016 (long-term period; **Figures 4**, **6**), supporting previous studies that suggest exposure and uptake of oil-derived PAHs from the

DWHOS occurred in offshore organisms (Murawski et al., 2014; Snyder et al., 2015; Romero et al., 2018). There are multiple sources of PAHs in the northern GoM (seeps, riverine discharges, continental runoff, coastal erosion, atmospheric deposition, and oil and gas exploration) (Park et al., 2001, 2002; Mitra and Bianchi, 2003; Tansel et al., 2011), with seeps as the most abundant among those sources (Ocean Studies Board and Marine Board, 2003). However, the DWHOS released an amount over seven times the average annual input of oil into the GoM, becoming the most important source of PAHs in summer to fall of 2010 (Murawski et al., 2014). As expected, most of the change in the composition of PAHs occurred for the low-molecular weight compounds (2–3 rings), abundant in oil that weathered and mixed over time with other sources (e.g., Mississippi river, natural seeps), as observed in 2015–2016. This inference is supported by similar abundances of retene between pre-pill and post-spill periods (**Figure 7**) indicating that natural sources of PAHs in the GoM do not explain the temporal trend observed in the composition of PAHs in the deep-sea cephalopod species studied.

The temporal trend for lipid content and PAH concentrations were also similar among the cephalopod species with significant changes over the 6-years of this study (**Figure 3**). However, the temporal trends observed in **Figure 3**, were not as expected for a one point-source contamination event, like the DWHOS

FIGURE 5 | Temporal variability of PAH concentrations in the mantle tissue of deep-sea cephalopods (species combined) collected in the northern Gulf of Mexico. Sampling years: pre-spill: 2010, post-spill: 2011, and long-term: 2015–2016. PAHs refer to the sum of 2–6 ring including alkylated homologs. Graph shows shaded boxes as the interquartile ranges, with horizontal lines indicating median values and whiskers representing 10th and 90th percentile. Blue circles denote mean values, and white circles denote outliers.

FIGURE 6 | Relative abundance (%) of PAH compounds in the mantle tissue of deep-sea cephalopods collected in the northern Gulf of Mexico. Sampling years: pre-spill: 2010, post-spill: 2011, and long-term: 2015–2016. Data are shown as mean ±SE.

FIGURE 7 | Temporal variation of PAH ratios in the mantle tissue of deep-sea cephalopods collected in the northern Gulf of Mexico. Sampling years: pre-spill: 2010, post-spill: 2011, and long-term: 2015–2016. Graph shows shaded boxes as the interquartile ranges, with horizontal lines indicating median values and whiskers representing 10th and 90th percentile. Blue circles denote mean values, and white circles denote outliers. Data are shown as mean ±SE.

in the summer of 2010. Lipid content was lower in 2011 (post-spill) relative to 2010 (pre-spill) for all species with samples collected in this year. Similarly, lipid-normalized PAH concentrations were lower in 2011 relative to 2010 for all species with samples collected in this year, except for *H. corona* (with similar concentrations for 2010 and 2011). The fact that in
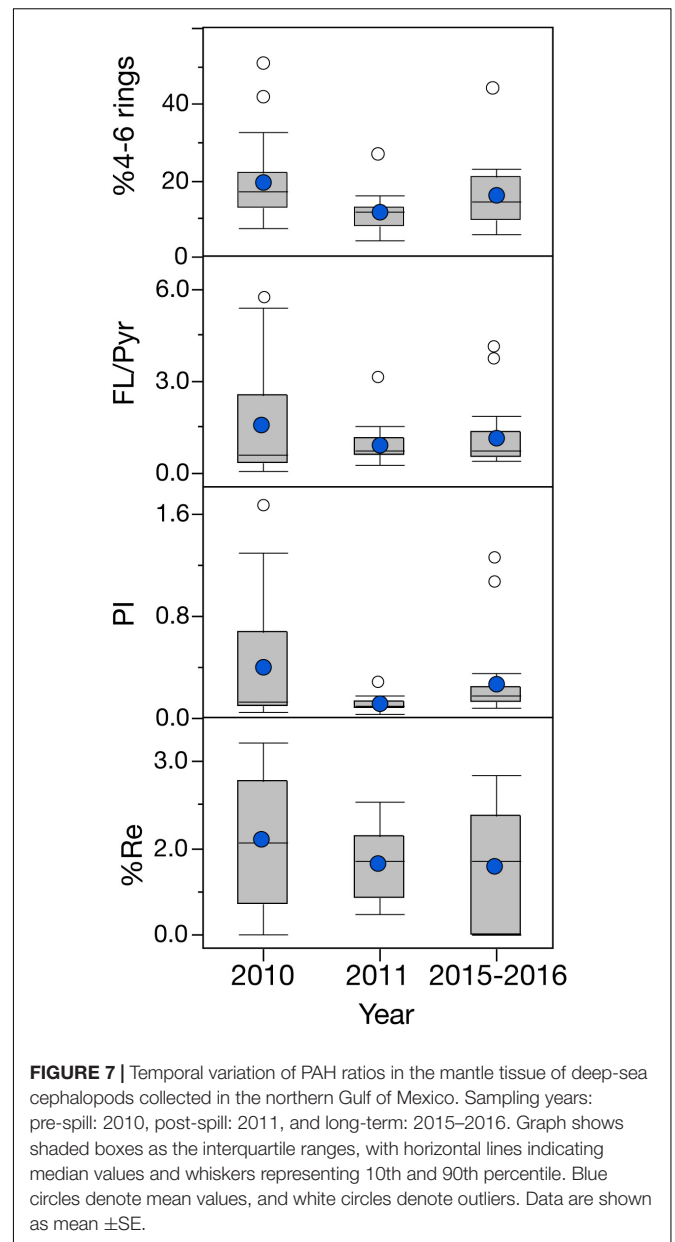
2011 PAH composition shows a shift in the source of PAHs but concentrations decreased, as well as lipid content, indicates that the temporal trends observed are secondary effects of the exposure to oil-residues from the DWHOS. We hypothesize that the lower lipid content in the cephalopod species observed in 2011 (post-spill) may be due to a change in dietary intake (decrease in prey availability) and/or dietary quality (e.g., fatty acids decrease in prey). Stable-isotope analysis of *J. diaphana*, *H. corona*, *O. banksii* and *L. atlantica* (Staudinger et al., in press, Richards et al., unpublished data) indicate that these species occupy multiple trophic positions, inhabiting a variety of ecological niches within the water column, all potentially affected by the DWHOS. Several studies demonstrated carbon from the DWHOS entered the planktonic and mesopelagic

food web after the spill (Chanton et al., 2012; Quintana-Rizzo et al., 2015) supporting the idea that potential prey species from different trophic levels were affected by oil-residues, which may have influenced the dietary intake of cephalopods. Moreover, several studies in shallower species, showed that dietary inputs can severely affect lipids, which are critical in cephalopod development (Navarro and Villanueva, 2003; Almansa et al., 2006; Guinot et al., 2013; Reis et al., 2016). Due to the hydrophobic properties of PAHs, significant changes in lipid content may also affect bioaccumulation of PAHs. The exception observed in the temporal trend for PAH concentrations in *H. corona* suggests other factors are important for bioaccumulation of PAHs in cephalopods. In this species, lower lipid content was observed post-spill (2011), albeit similar PAH concentrations pre- and post-spill (2010 and 2011), and 84% higher concentrations in the long-term period (2015–2016). Of all the species studied, *H. corona* is the only one that lives in the mesopelagic zone and does not migrate to the surface to feed (**Supplementary Table S1**). Oil-residues have been observed in the water column years after the spill (Walker et al., 2017), probably from resuspension of contaminated sediments (Romero et al., 2017; Diercks et al., 2018). It is possible that the dietary intake for *H. corona* was affected like the other species studied (**Figure 3**), but with an extended period of exposure to oil-residues persistent at depth. This is supported by elevated PAH concentrations observed in the long-term period (2015–2016).

Collectively, PAH composition trends in the deep-sea cephalopod species studied suggest an episodic exposure to petrogenic PAHs that occurred after the pre-spill sampling campaign in 2010 and continued through 2015–2016. Exposure to oil-derived PAHs occurred after the DWHOS, but secondary effects, including potential trophic-web effects, may have influenced the lipid content and PAH levels post-spill (2011). It appears that exposure to oil-derived residues is longer than expected in the pelagic deep-sea environment, as observed from the same event in mesopelagic fishes (Romero et al., 2018). This phenomenon may have disturbed the deep-sea environment via the food web, as indicated by the temporal trend observed in cephalopod species. Due to the important role of lipids on the physiology of cephalopods (Reis et al., 2016), future studies should evaluate lipid composition in relation to dietary intake and organic contaminants. Also, studies should cover longer periods for a better understating of the persistence of organic pollutants at depth and impacts to pelagic communities from different trophic levels.

DATA AVAILABILITY STATEMENT

Data are publicly available through the Gulf of Mexico Research Initiative and Data Cooperative (GRIIDC) at https://data.gulfresearchinitiative.org (doi: 10.7266/XN8NE9DW).

ETHICS STATEMENT

The animal study was reviewed and approved by the IACUC USF.

AUTHOR CONTRIBUTIONS

IR carried out the laboratory and data analyses, and wrote the manuscript including figures and tables. HJ and MV collected the samples and identified specimens to species levels, as well as contributing to the manuscript by revising, editing, and adding references and comments.

FUNDING

ACKNOWLEDGMENTS

SUPPLEMENTARY MATERIAL

The Supplementary Material for this article can be found online at: https://www.frontiersin.org/articles/10.3389/fmars.2020.00054/full#supplementary-material

FIGURE S1 | % change in the composition of PAHs in 2011 (post-spill) and 2015–2016 (long-term period) relative to 2010 (pre-spill) in the mantle tissue of deep-sea cephalopods collected in the northern Gulf of Mexico. Graph shows bars as the % difference of normalized concentrations by total PAHs between sampling periods (2011 minus 2010; 2015–2016 minus 2010). Values >0 indicate an increase in the abundance of individual PAHs, while values <0 indicate a decrease in the abundance of individual PAHs.

FIGURE S2 | Temporal variability of PAH concentrations in the mantle tissue of deep-sea cephalopods (species combined) collected in the northern Gulf of Mexico. Sampling years: pre-spill: 2010, post-spill: 2011, and long-term: 2015–2016. PAHs refer to the sum of 2–6 ring including alkylated homologs. Graph shows shaded boxes as the interquartile ranges, with horizontal lines indicating median values and whiskers representing 10th and 90th percentile. Blue circles denote mean values, and white circles denote outliers.

FIGURE S3 | Relative abundance (%) of PAH compounds in the mantle tissue of deep-sea cephalopods collected in three areas in northern Gulf of Mexico. Sampling years: pre-spill: 2010, post-spill: 2011, and long-term: 2015–2016. Data are shown as mean ±SE.

TABLE S1 | Ecological characteristics of deep-sea cephalopod species from the northern GoM.

REFERENCES

Adhikari, P. L., Wong, R. L., and Overton, E. B. (2017). Application of enhanced gas chromatography/triple quadrupole mass spectrometry for monitoring petroleum weathering and forensic source fingerprinting in samples impacted by the deepwater Horizon oil spill. *Chemosphere* 184, 939–950. doi: 10.1016/j.chemosphere.2017.06.077

Almansa, E., Domingues, P., Sykes, A., Tejera, N., Lorenzo, A., and Andrade, J. P. (2006). The effects of feeding with shrimp or fish fry on growth and mantle lipid composition of juvenile and adult cuttlefish (*Sepia officinalis*). *Aquaculture* 256, 403–413. doi: 10.1016/j.aquaculture.2006.02.025

Beriro, D. J., Vane, C. H., Cave, M. R., and Nathanail, C. P. (2014). Effects of drying and comminution type on the quantification of polycyclic aromatic hydrocarbons (PAH) in a homogenised gasworks soil and the implications for human health risk assessment. *Chemosphere* 111, 396–404. doi: 10.1016/j.chemosphere.2014.03.077

Brooks, G. R., Larson, R. A., Schwing, P. T., Romero, I., Moore, C., Reichart, G. J., et al. (2015). Sedimentation pulse in the NE Gulf of Mexico following the 2010 DWH blowout. *PLoS One* 10:132341. doi: 10.1371/journal.pone.0132341

Chanton, J. P., Cherrier, J., Wilson, R. M., Sarkodee-Adoo, J., Bosman, S., Mickle, A., et al. (2012). Radiocarbon evidence that carbon from the Deepwater Horizon Spill entered the planktonic food web of the Gulf of Mexico. *Environ. Res. Lett.* 7, 1–4. doi: 10.1088/1748-9326/7/4/045303

Chanton, J. P., Giering, S. L. C., Bosman, S. H., Rogers, K. L., Sweet, J., Asper, V. L., et al. (2018). Isotopic composition of sinking particles : oil effects, recovery and baselines in the Gulf of Mexico, 2010-2015. *Elem. Sci. Anthr.* 6, 2010–2015. doi: 10.1525/elementa.298

Corrales, X., Coll, M., Tecchio, S., María, J., Mario, A., and Palomera, I. (2015). Ecosystem structure and fishing impacts in the northwestern Mediterranean Sea using a food web model within a comparative approach. *J. Mar. Syst.* 148, 183–199. doi: 10.1016/j.jmarsys.2015.03.006

Daly, K. L., Passow, U., Chanton, J., and Hollander, D. (2016). Assessing the impacts of oil-associated marine snow formation and sedimentation during and after the Deepwater Horizon oil spill. *Biochem. Pharmacol.* 13, 18–33. doi: 10.1016/j.ancene.2016.01.006

Davis, R. W., Jaquet, N., Gendron, D., Markaida, U., Bazzino, G., and Gilly, W. (2007). Diving behavior of sperm whales in relation to behavior of a major prey species, the jumbo squid, in the Gulf of California, Mexico. *Mar. Ecol. Prog. Ser.* 333, 291–302. doi: 10.3354/meps333291

Davison, P. C. Jr., Koslow, J. A., and Barlow, J. (2013). Carbon export mediated by mesopelagic fishes in the northeast Pacific Ocean. *Prog. Oceanogr.* 116, 14–30. doi: 10.1016/j.pocean.2013.05.013

Diercks, A., Dike, C., Asper, V. L., Dimarco, S. F., and Jeffrey, P. (2018). Scales of seafloor sediment resuspension in the northern Gulf of Mexico. *Elem. Sci. Anthr.* 1, 1–28. doi: 10.1525/elementa.285

Dietrich, J. C., Trahan, C. J., Howard, M. T., Fleming, J. G., Weaver, R. J., Tanaka, S., et al. (2012). Surface trajectories of oil transport along the Northern Coastline of the Gulf of Mexico. *Cont. Shelf Res.* 41, 17–47. doi: 10.1016/j.csr.2012.03.015

Fisher, C. R., Montagna, P. A., and Sutton, T. T. (2016). How did the Deepwater Horizon oil spill impact deep-sea ecosystems? *Oceanography* 29, 182–195. doi: 10.5670/oceanog.2016.82

Fitzgerald, T. P., and Gohlke, J. M. (2014). Contaminant levels in gulf of Mexico reef fish after the deepwater horizon oil spill as measured by a fishermen-led testing program. *Environ. Sci. Technol.* 48, 1993–2000. doi: 10.1021/es4051555

Gomes, F., Oliveira, M., Ramalhosa, M. J., Delerue-matos, C., and Morais, S. (2013). Polycyclic aromatic hydrocarbons in commercial squids from different geographical origins : levels and risks for human consumption. *Food Chem. Toxicol.* 59, 46–54. doi: 10.1016/j.fct.2013.05.034

Graham, W. M., Condon, R. H., Carmichael, R. H., D'Ambra, I., Patterson, H. K., Linn, L. J., et al. (2010). Oil carbon entered the coastal planktonic food web during the Deepwater Horizon oil spill. *Environ. Res. Lett.* 5:045301. doi: 10.1088/1748-9326/5/4/045301

Guinot, D., Monroig, O., Navarro, J. C., Varo, I., Amat, F., and Hontoria, F. (2013). Enrichment of *Artemia metanauplii* in phospholipids and essential fatty acids as a diet for common octopus (Octopus vulgaris) paralarvae. *Aquac. Nutr.* 19, 837–844. doi: 10.1111/anu.12048

Harding, V., Camp, J., Morgan, L. J., and Gryko, J. (2016). Oil residue contamination of continental shelf sediments of the Gulf of Mexico. *Mar. Pollut. Bull.* 113, 488–495. doi: 10.1016/j.marpolbul.2016.07.032

Hazen, T. C., Dubinsky, E. A., DeSantis, T. Z., Andersen, G. L., Piceno, Y. M., Singh, N., et al. (2010). Deep-sea oil plume enriches indigenous oil-degrading bacteria. *Science* 330, 204–208. doi: 10.1126/science.1195979

Hooper, T., and Parrish, C. C. (2009). Profiling neutral lipids in individual fish larvae by using shortcolumn gas chromatography with flame ionization detection. *Limnol. Oceanogr. Methods* 7, 411–418. doi: 10.4319/lom.2009.7.411

Hoving, H. J. T., and Robison, B. H. (2017). The pace of life in deep-dwelling squids. *Deep Res. I* 126, 40–49. doi: 10.1016/j.dsr.2017.05.005

Hudson, J. M., Steinberg, D. K., Sutton, T. T., Graves, J. E., and Latour, R. J. (2014). Myctophid feeding ecology and carbon transport along the northern Mid-Atlantic Ridge. *Deep Res. I* 93, 104–116. doi: 10.1016/j.dsr.2014.07.002

Irigoien, X., Klevjer, T. A., Rostad, A., Martinez, U., Boyra, G., Acuna, J. L., et al. (2014). Large mesopelagic fishes biomass and trophic efficiency in the open ocean. *Nat. Commun.* 5:4271. doi: 10.1038/ncomms4271

Judkins, H., Arbuckle, S., Vecchione, M., and Martinez, A. (2015). Cephalopods in the potential prey field of sperm whales (Physeter macrocephalus) (Cetacea : Physeteridae) in the northern Gulf of Mexico. *J. Nat. Hist.* 49, 37–41. doi: 10.1080/00222933.2013.802045

Judkins, H., Vecchione, M., Cook, A., and Sutton, T. (2017). Diversity of midwater cephalopods in the northern Gulf of Mexico : comparison of two collecting methods. *Mar. Biodivers.* 47, 647–657. doi: 10.1007/s12526-016-0597-8

Lacoue-Labarthe, T., Le PAbic, C., and Bustamante, P. (2016). Ecotoxicology of early-life stages in the common cuttlefish. *Vie Milieu* 66, 65–79.

Lalas, C., and Webster, T. (2014). Contrast in the importance of arrow squid as prey of male New Zealand sea lions and New Zealand fur seals at The Snares, subantarctic New Zealand. *Mar. Biol.* 161, 631–643. doi: 10.1007/s00227-013-2366-6

Logan, J. M., Toppin, R., Smith, S., Galuardi, B., Porter, J., and Lutcavage, M. (2013). Contribution of cephalopod prey to the diet of large pelagic fish predators in the central North Atlantic Ocean. *Deep Res. II* 95, 74–82. doi: 10.1016/j.dsr2.2012.06.003

MacDonald, I. R., Garcia-Pineda, O., Beet, A., Daneshgar, A., Feng, L., Graettinger, G., et al. (2015). Natural and unnatural oil slicks in the Gulf of Mexico. *J. Geophys. Res. Ocean* 120, 3896–3912.

Mitra, S., and Bianchi, T. (2003). A preliminary assessment of polycyclic aromatic hydrocarbon distributions in the lower Mississippi River and Gulf of Mexico. *Mar. Chem.* 82, 273–288. doi: 10.1016/S0304-4203(03)00074-4

Mitra, S., Bianchi, T. S., Mckee, B. A., and Sutula, M. (2002). Black carbon from the mississippi river: quantities, sources, and potential implications for the global carbon cycle. *Environ. Sci. Technol.* 36, 2296–2302. doi: 10.1021/es015834b

Murawski, S. A., Fleeger, J. W., Patterson, W. F., Hu, C., Daly, K., Romero, I., et al. (2016). How did the Deepwater Horizon oil spill affect coastal and continental shelf ecosystems of the Gulf of Mexico? *Oceanography* 29, 160–173. doi: 10.5670/oceanog.2016.80

Murawski, S. A., Hogarth, W. T., Peebles, E. B., and Barbeiri, L. (2014). Prevalence of external skin lesions and polycyclic aromatic hydrocarbon concentrations in Gulf of Mexico fishes, post-Deepwater Horizon. *Trans. Am. Fish. Soc.* 143, 37–41. doi: 10.1080/00028487.2014.911205

Navarro, J. C., and Villanueva, R. (2003). The fatty acid composition of Octopus vulgaris paralarvae reared with live and inert food : deviation from their natural fatty acid profile. *Aquaculture* 219, 613–631. doi: 10.1016/s0044-8486(02)00311-3

Ocean Studies Board and Marine Board (2003). *Oil in the Sea III. Inputs, Fates, and Effects*. Washington, D.C: National Academies Press.

Park, J., Wade, T. L., and Sweet, S. (2001). Atmospheric distribution of polycyclic aromatic hydrocarbons and deposition to Galveston Bay, Texas, USA. *Atmos. Environ.* 35, 3241–3249. doi: 10.1016/s1352-2310(01)00080-2

Park, J., Wade, T. L., and Sweet, S. T. (2002). Atmospheric deposition of PAHs, PCBs, and organochlorine pesticides to Corpus Christi Bay, Texas. *Atmos. Environ.* 36, 1707–1720. doi: 10.1016/s1352-2310(01)00586-6

Quintana-Rizzo, E., Torres, J. J., Ross, S. W., Romero, I., Watson, K., Goddard, E., et al. (2015). δ13C and δ15N in deep-living fishes and shrimps after the Deepwater Horizon oil spill Gulf of Mexico. *Mar. Pollut. Bull.* 94, 241–250. doi: 10.1016/j.marpolbul.2015.02.002

Reis, D. B., Acosta, N. G., Almansa, E., Tocher, D. R., Andrade, J. P., Sykes, A. V., et al. (2016). Composition and metabolism of phospholipids in Octopus vulgaris and *Sepia officinalis* hatchlings. *Comp. Biochem. Physiol. B Biochem. Mol. Biol.* 200, 62–68. doi: 10.1016/j.cbpb.2016.06.001

Rodrigo, A. P., and Costa, P. M. (2017). The Role of the cephalopod digestive gland in the storage and detoxification of marine pollutants. *Front. Physiol.* 8:232. doi: 10.3389/fphys.2017.00232

Romeo, T., Battaglia, P., and Peda, C. (2012). Pelagic cephalopods of the central Mediterranean Sea determined by the analysis of the stomach content of large fish predators. *Helgo. Mar. Res.* 66, 295–306. doi: 10.1007/s10152-011-0270-3

Romero, I. C., Özgökmen, T., Snyder, S., Schwing, P., O'Malley, B. J., Beron-Vera, F. J., et al. (2016). Tracking the hercules 265 marine gas well blowout in the Gulf of Mexico. *J. Geophys. Res. Ocean* 121, 706–724. doi: 10.1002/2015JC011037

Romero, I. C., Schwing, P. T., Brooks, G. R., Larson, R. A., Hastings, D. W., Flower, B. P., et al. (2015). Hydrocarbons in deep-sea sediments following the 2010 Deepwater Horizon Blowout in the Northeast Gulf of Mexico. *PLoS One* 10:128371. doi: 10.1371/journal.pone.0128371

Romero, I. C., Sutton, T., Carr, B., Quintana-Rizzo, E., Ross, S. W., Hollander, D. J., et al. (2018). A decadal assessment of polycyclic aromatic hydrocarbons in mesopelagic fishes from the Gulf of Mexico reveals exposure to oil-derived sources. *Environ. Sci. Technol.* 52, 10985–10996. doi: 10.1021/acs.est.8b02243

Romero, I. C., Toro-farmer, G., Diercks, A., Schwing, P., Muller-Karger, F., Murawski, S., et al. (2017). Large-scale deposition of weathered oil in the Gulf of Mexico following a deep-water oil spill. *Environ. Pollut.* 228, 179–189. doi: 10.1016/j.envpol.2017.05.019

Ryerson, T. B., Camilli, R., Kessler, J. D., Kujawinski, E. B., Reddy, C. M., Valentine, D. L., et al. (2012). Chemical data quantify Deepwater Horizon hydrocarbon flow rate and environmental distribution. *Proc. Natl. Acad. Sci. U.S.A.* 109, 20246–20253. doi: 10.1073/pnas.1110564109

Salman, A., and Karakulak, F. S. (2019). Cephalopods in the diet of albacore, *Thunnus alalunga*, from the eastern mediterranean. *J. Mar. Biol. Assoc. U. K.* 89, 635–640. doi: 10.1017/S0025315408002555

Semedo, M., Oliveira, M., Gomes, F., Reis-henriques, M. A., Delerue-matos, C., Morais, S., et al. (2014). Seasonal patterns of polycyclic aromatic hydrocarbons in digestive gland and arm of octopus (Octopus vulgaris) from the Northwest Atlantic. *Sci. Total Environ.* 481, 488–497. doi: 10.1016/j.scitotenv.2014.02.088

Sloan, C. A., Brown, D. W., Pearce, R. W., Boyer, R. H. Bolton, J. L., Burrows, D. G., et al. (2004). Extraction, cleanup, and gas chromatography/mass spectrometry analysis of sediments and tissues for organic contaminants. *U.S. Dept. Commer. NOAA Tech. Memo. NMFS-NWFSC-59*, 47.

Snyder, S. M., Pulster, E. L., Wetzel, D. L., and Murawski, S. A. (2015). PAH exposure in Gulf of Mexico demersal fishes, post-deepwater horizon. *Environ. Sci. Technol.* 49, 8786–8795. doi: 10.1021/acs.est.5b01870

Sorensen, L., Meier, S., and Mjos, S. A. (2016). Application of gas chromatography/tandem mass spectrometry to determine a wide range of petrogenic alkylated polycyclic aromatic hydrocarbons in biotic samples. *Rapid Commun. Mass Spectr.* 30, 2052–2058. doi: 10.1002/rcm.7688

Southall, B. L., Benoit-bird, K. J., Moline, M. A., and Moretti, D. (2019). Quantifying deep-sea predator– prey dynamics: implications of biological heterogeneity for beaked whale conservation. *J. Appl. Ecol.* 56, 1040–1049. doi: 10.1111/1365-2664.13334

Steinberg, D. K., Cope, J. S., Wilson, S. E., and Kobari, T. (2008). A comparison of mesopelagic mesozooplankton community structure in the subtropical and subarctic North Pacific Ocean. *Deep Res. II* 55, 1615–1635. doi: 10.1016/j.dsr2.2008.04.025

Steinberg, D. K., and Landry, M. R. (2017). Zooplankton and the ocean carbon cycle. *Annu. Rev. Earth Planet. Sci.* 9, 413–444. doi: 10.1146/annurev-marine-010814-015924

Stewart, J. S., Hazen, E. L., Bograd, S. J., Jarrett, E. K., Gilly, W. F., and Robison, B. H. (2014). Combined climate- and prey-mediated range expansion of humboldt squid (Dosidicus gigas), a large marine predator in the California Current System. *Glob. Chang. Biol.* 20, 1832–1843. doi: 10.1111/gcb.12502

Tansel, B., Fuentes, C., Sanchez, M., Predoi, K., and Acevedo, M. (2011). Persistence profile of polyaromatic hydrocarbons in shallow and deep Gulf waters and sediments: effect of water temperature and sediment-water partitioning characteristics. *Mar. Pollut. Bull.* 62, 2659–2665. doi: 10.1016/j.marpolbul.2011.09.026

Taucher, J., Stange, P., Algueró-muñiz, M., Bach, L. T., Nauendorf, A., Kolzenburg, R., et al. (2018). In situ camera observations reveal major role of zooplankton in modulating marine snow formation during an upwelling-induced plankton bloom. *Prog. Oceanogr.* 164, 75–88. doi: 10.1016/j.pocean.2018.01.004

U.S. District Court, (2015). *Findings of Facts and Conclusions of Law - Phase 2 Trial*. Coffeyville, KS: U.S. District Court.

Unger, M. A., Harvey, E., Vadas, G. G., and Vecchione, M. (2008). Persistent pollutants in nine species of deep-sea cephalopods. *Mar. Pollut. Bull.* 56, 2003–2005.

van Eenennaam, J. S., Rahsepar, S., Radoviæ, J. R., Oldenburg, T. B. P., Wonink, J., Langenhoff, A. A. M., et al. (2018). Marine snow increases the adverse effects of oil on benthic invertebrates. *Mar. Pollut. Bull.* 126, 339–348. doi: 10.1016/j.marpolbul.2017.11.028

Wade, T. L., Sericano, J. L., Sweet, S. T., Knap, A. H., and Guinasso, N. L. (2016). Spatial and temporal distribution of water column total polycyclic aromatic hydrocarbons (PAH) and total petroleum hydrocarbons (TPH) from the Deepwater Horizon (Macondo) incident. *Mar. Pollut. Bull.* 103, 286–293. doi: 10.1016/j.marpolbul.2015.12.002

Walker, B. D., Druffel, E. R. M., Kolasinski, J., Roberts, B. J., Xu, X., and Rosenheim, B. E. (2017). Stable and radiocarbon isotopic composition of dissolved organic matter in the Gulf of Mexico. *Geophys. Res. Lett.* 44, 8424–8434. doi: 10.1002/2017GL074155

Wang, Z., and Fingas, M. F. (2003). Development of oil hydrocarbon fingerprinting and identification techniques. *Mar. Pollut. Bull.* 47, 423–452. doi: 10.1016/S0025-326X(03)00215-7

Yan, B., Passow, U., Chanton, J. P., Nöthig, E.-M., Asper, V., Sweet, J., et al. (2016). Sustained deposition of contaminants from the Deepwater Horizon spill. *Proc. Natl. Acad. Sci. U.S.A.* 113, E3332–E3340. doi: 10.1073/pnas.1513156113

Young, J. W., Guest, M. A., Lansdell, M., Phleger, C. F., and Nichols, P. D. (2010). Discrimination of prey species of juvenile swordfish *Xiphias gladius* (Linnaeus, 1758) using signature fatty acid analyses. *Prog. Oceanogr.* 86, 139–151. doi: 10.1016/j.pocean.2010.04.028